QED corrections to the radiative recombination of an electron with a bare nucleus

V. M. Shabaev,[1,2] V. A. Yerokhin,[2,3] T. Beier,[4] and J. Eichler[2]
[1]*Department of Physics, St. Petersburg State University, Oulianovskaya 1, Petrodvorets, St. Petersburg 198904, Russia*
[2]*Bereich Theoretische Physik, Hahn-Meitner-Institut, 14109 Berlin, Germany*
[3]*Institute for High Performance Computing and Data Bases, Fontanka 118, St. Petersburg 198005, Russia*
[4]*Fysik och Teknisk Fysik, Chalmers Tekniska Högskola och Göteborgs Universitet, SE-412 96 Göteborg, Sweden*
(Received 27 October 1999; published 18 April 2000)

Complete formulas for the QED corrections of the first order in α to the radiative recombination of an electron with a bare nucleus are derived. An analysis of the ultraviolet and infrared divergences is presented. Application of the formulas to the radiative electron capture process is discussed. Numerical results are presented for the vacuum-polarization correction evaluated in the Uehling approximation and for a part of the self-energy correction.

PACS number(s): 12.20.Ds, 11.80.−m, 34.80.Kw

I. INTRODUCTION

In an energetic collision between a highly charged high-Z ion and a low-Z target atom, an electron may be captured by the projectile, while a simultaneously emitted photon carries away the excess energy and momentum. This process is denoted as radiative electron capture (REC). Since a loosely bound target electron can be considered as quasifree, it is essentially equivalent to radiative recombination (RR) or its time-reversed analogon, the photoelectric effect. At the GSI Darmstadt [1,2], reactions of this type have been extensively studied using bare projectiles up to U^{92+} with energies up to several hundred MeV/u. The relativistic theory of REC was considered in detail in Refs. [3–5], and the results of this theory are in excellent agreement with experiment. In particular, the spin-flip contribution to REC, calculated in Refs. [3–5], was recently identified in angular-differential measurements [6].

In view of the increasing experimental accuracy and the well-defined theoretical description, it is tempting to search for quantum electrodynamic (QED) effects supplementing the existing theory [3–5]. Indeed, heavy ions are good systems for testing QED effects in strong electric fields. However, until now, such effects in heavy ions, for example, the Lamb shift, were investigated only for bound states (see Ref. [7], and references therein). On the other hand, QED corrections to the photoeffect were considered only to the lowest order in αZ [8,9]. Since calculations based on an αZ expansion are not valid for high-Z systems, it is desirable to perform calculations for the complete αZ dependence.

A systematic QED theory of the RR process has been worked out in [10]. In the present paper, we apply this theory to derive the formulas for the QED corrections of the first order in α to radiative recombination of an electron with a bare nucleus. We analyze the infrared and ultraviolet divergences and discuss the application of these formulas to the REC process. We calculate the vacuum-polarization correction using the Uehling approximation and a part of the self-energy correction. Relativistic units ($\hbar=c=1$) are used in the paper.

II. BASIC FORMULAS

We consider the radiative recombination of an electron with momentum $\mathbf{p}_i$ and polarization μ_i with a bare nucleus which is put at the origin of the coordinate frame. This corresponds to the projectile system if we study the radiative recombination of a free target electron with a bare heavy projectile. The differential cross section of this process is given by

$$d\sigma=\frac{(2\pi)^4}{v_i}|\tau|^2\delta(\varepsilon_a+k_f^0-p_i^0)\,d\mathbf{k}_f, \tag{1}$$

where $p_i^0=\sqrt{\mathbf{p}_i^2+m^2}$ is the energy of the incident electron, ε_a is the energy of the final state a of the one-electron atom, $k_f=(k_f^0,\mathbf{k}_f)$ with k_f^0 and $\mathbf{k}_f$ being the photon energy and momentum, respectively, v_i is the velocity of the incident electron in the nucleus frame, and τ is the amplitude of the process which is connected with the S-matrix element by

$$\langle k_f,\boldsymbol{\epsilon}_f;a|S|p_i,\mu_i\rangle=2\pi i\,\delta(\varepsilon_a+k_f^0-p_i^0)\,\tau. \tag{2}$$

Here $\boldsymbol{\epsilon}_f=(0,\boldsymbol{\epsilon}_f)$ is the photon polarization and $p_i=(p_i^0,\mathbf{p}_i)$. According to the standard reduction technique (see, e.g., Ref. [11]), we have

$$\begin{aligned}\langle k_f,\boldsymbol{\epsilon}_f;a|S|p_i,\mu_i\rangle&=\langle a|a_{\rm out}(k_f,\boldsymbol{\epsilon}_f)b_{\rm in}^{\dagger}(p_i,\mu_i)|0\rangle\\&=(-iZ_3^{-1/2})(-iZ_2^{-1/2})\\&\quad\times\int d^4y\,d^4z\,\frac{\boldsymbol{\epsilon}_f^{\nu}\exp(ik_f\cdot y)}{\sqrt{2k_f^0(2\pi)^3}}\\&\quad\times\langle a|Tj_{\nu}(y)\bar{\psi}(z)|0\rangle(-i\overleftarrow{\partial}_z-m)\\&\quad\times\frac{u(p_i,\mu_i)\exp(-ip_i\cdot z)}{\sqrt{\frac{p_i^0}{m}(2\pi)^3}},\end{aligned} \tag{3}$$

where T is the time-ordering operator, $a\cdot b\equiv a^{\nu}b_{\nu}\psi(x)$ is the electron-positron field operator in the Heisenberg representation, $j_{\nu}(y)=(e/2)[\bar{\psi}(y),\gamma_{\nu}\psi(y)]$ is the electron-positron current operator, Z_2 and Z_3 are the renormalization constants, and $u(p_i,\mu_i)$ is the free wave function of the incident electron normalized by the condition $\bar{u}u=1$.

Equation (3) is rather formal and cannot be used for the direct calculation of the amplitude if $|a\rangle$ is a bound atomic state. To calculate this amplitude by perturbation theory we need a special technique. Such a technique was developed in Ref. [10] for the general case of a few-electron atom. In the present paper we apply this technique to the case of a bare nucleus in the initial state and an one-electron atom in the final state. In this case the amplitude of the process is calculated by

$$\langle k_f,\epsilon_f;a|S|p_i,\mu_i\rangle = -\delta(\varepsilon_a+k_f^0-p_i^0) \times (Z_2Z_3)^{-1/2}\oint_\Gamma dE\, g_{\gamma_f,a;e_i}(E,p_i^0) \times\left[\frac{1}{2\pi i}\oint_\Gamma dE\, g_a(E)\right]^{-1/2}. \tag{4}$$

Here Γ is a contour in the complex E plane which surrounds the level a and does not surround other levels and it is assumed to be counterclockwise. The functions $g_a(E)$ and $g_{\gamma_f,a;e_i}(E,p^0)$ are defined by

$$g_a(E)\,\delta(E'-E)=\frac{2\pi}{i}\int d\mathbf{x}d\mathbf{y}\,\psi_a^\dagger(\mathbf{x})G(E',E,\mathbf{x},\mathbf{y})\,\gamma^0\psi_a(\mathbf{y}), \tag{5}$$

$$g_{\gamma_f,a;e_i}(E,p^0)\,\delta(E+k^0-p^0) = \int d\mathbf{x}\psi_a^\dagger(\mathbf{x})G_{\gamma_f,e_i}(k^0,E,p^0,\mathbf{x}), \tag{6}$$

$\psi_a(\mathbf{x})$ is the wave function of the final state of the one-electron atom, G and G_{γ_f,e_i} are defined in the Heisenberg representation by the equations

$$G(E',E,\mathbf{x},\mathbf{y})=\frac{1}{(2\pi)^2}\int_{-\infty}^{\infty}dx^0dy^0\exp(iE'x^0-iEy^0) \times\langle 0|T\psi(x)\overline{\psi}(y)|0\rangle, \tag{7}$$

$$G_{\gamma_f,e_i}(k^0,E,p^0,\mathbf{x})=-\frac{1}{2\pi}\int_{-\infty}^{\infty}dx^0\exp(iEx^0)\int d^4yd^4z\exp(ik^0y^0-ip^0z^0)\frac{\epsilon_f^\nu\exp(-i\mathbf{k}_f\cdot\mathbf{y})}{\sqrt{2k_f^0(2\pi)^3}} \times\langle 0|T\psi(x)j_\nu(y)\overline{\psi}(z)|0\rangle(-i\tilde{\partial}_z-m)\frac{u(p_i,\mu_i)\exp(i\mathbf{p}_i\cdot\mathbf{z})}{\sqrt{\frac{p_i^0}{m}(2\pi)^3}}. \tag{8}$$

As is evident from these equations, G is simply the full one-electron Green function and G_{γ_f,e_i} is the Green function describing the radiative recombination process. Both G and G_{γ_f,e_i} are constructed by perturbation theory after the transition to the interaction representation in Eqs. (7) and (8) and using Wick's theorem. The Feynman rules for G and G_{γ_f,e_i} are given in Ref. [10]. G_{γ_f,e_i} differs from G by presence of the outgoing photon line and by insertion of the incident electron wave function instead of the initial electron propagator.

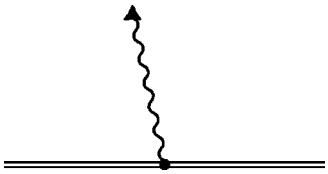

FIG. 1. The radiative recombination of an electron with a bare nucleus in the zeroth-order approximation. The double line denotes the electron propagating in the Coulomb field of the nucleus. The wavy line ended by the arrow denotes the emitted photon.

III. ZEROTH-ORDER APPROXIMATION

To the zeroth order we have the diagram shown in Fig. 1. The formula (4) gives

$$\langle k_f,\epsilon_f;a|S^{(0)}|p_i,\mu_i\rangle = -\delta(\varepsilon_a+k_f^0-p_i^0) \times\oint_\Gamma dE\, g^{(0)}_{\gamma_f,a;e_i}(E,p_i^0), \tag{9}$$

where the superscript indicates the order in α. Here we have taken into account that

$$\frac{1}{2\pi i}\oint_\Gamma dE\, g_a^{(0)}(E)=\frac{1}{2\pi i}\oint_\Gamma dE\,\frac{1}{E-\varepsilon_a}=1. \tag{10}$$

According to the Feynman rules from Ref. [10], we have

$$G^{(0)}_{\gamma_f,e_i}(k^0,E,p^0,\mathbf{x})=\int d\mathbf{y}\frac{i}{2\pi}S(E,\mathbf{x},\mathbf{y})(-ie\gamma^\nu 2\pi) \times\delta(E+k^0-p^0)A^*_{f,\nu}(\mathbf{y})\psi_{p_i\mu_i(+)}(\mathbf{y}), \tag{11}$$

where

$$S(\omega,\mathbf{x},\mathbf{y})=\sum_n \frac{\psi_n(\mathbf{x})\bar{\psi}_n(\mathbf{y})}{\omega-\varepsilon_n(1-i0)} \tag{12}$$

is the electron propagator in the Coulomb field of the nucleus,

$$A^\nu_f(\mathbf{x})=\frac{\epsilon^\nu_f \exp(i\mathbf{k}_f\cdot\mathbf{x})}{\sqrt{2k^0_f(2\pi)^3}} \tag{13}$$

is the wave function of the outgoing photon, and $\psi_{p_i\mu_i(+)}(\mathbf{x})$ is the wave function of the incoming electron in the Coulomb field defined by the equation (see Ref. [10] for details)

$$\psi_{p_i\mu_i(+)}=\frac{u(p_i,\mu_i)\exp(i\mathbf{p}_i\cdot\mathbf{x})}{\sqrt{\frac{p^0_i}{m}(2\pi)^3}}+[p^0_i-H_0(1-i0)]^{-1}$$

$$\times V_C\psi_{p_i\mu_i(+)}. \tag{14}$$

Here $H_0=\alpha\mathbf{p}+\beta m$ is the free-electron Hamiltonian and V_C is the Coulomb field of the nucleus. The apparent expressions for $\psi_{p_i\mu_i(+)}$ are given, e.g., in Ref. [4]. Substituting the expression (11) into the Eq. (6), we obtain

$$g^{(0)}_{\gamma_f,a;e_i}(E,p^0)=\frac{\langle a|e\alpha^\nu A^*_{f,\nu}|p_i,\mu_i\rangle}{E-\varepsilon_a}. \tag{15}$$

Equations (9) and (15) yield

$$\langle k_f,\epsilon_f;a|S^{(0)}|p_i,\mu_i\rangle=-2\pi i\,\delta(\varepsilon_a+k^0_f-p^0_i)$$

$$\times\langle a|e\alpha^\nu A^*_{f,\nu}|p_i,\mu_i\rangle \tag{16}$$

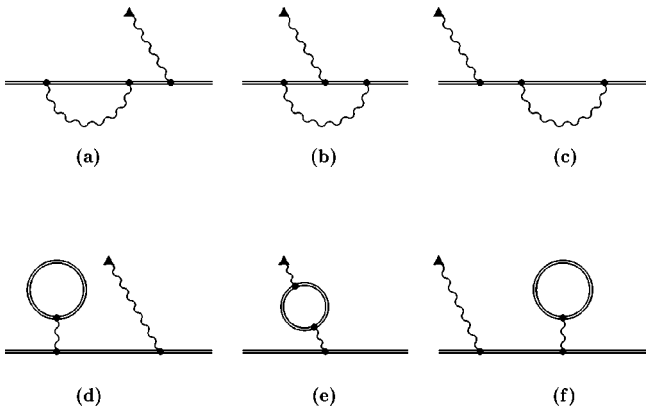

FIG. 2. The first-order QED corrections to the radiative recombination of an electron with a bare nucleus.

or according to the definition (2)

$$\tau^{(0)}=-\langle a|e\alpha^\nu A^*_{f,\nu}|p_i,\mu_i\rangle=\langle a|e\boldsymbol{\alpha}\cdot\mathbf{A}^*_f|p_i,\mu_i\rangle. \tag{17}$$

The corresponding cross section is

$$\frac{d\sigma^{(0)}}{d\Omega_f}=\frac{(2\pi)^4}{v_i}\mathbf{k}^2_f|\tau^{(0)}|^2. \tag{18}$$

IV. QED CORRECTIONS OF THE FIRST ORDER IN α

The QED corrections of first order in α are defined by the diagrams shown in Fig. 2. Let us consider in detail the derivation of the formal expressions for the self-energy (SE) corrections [diagrams (a)–(c)]. The formula (4) gives in the order under consideration

$$\langle k_f,\epsilon_f;a|S^{(1)}|p_i,\mu_i\rangle=-\delta(\varepsilon_a+k^0_f-p^0_i)\Bigg[\oint_\Gamma dE g^{(1)}_{\gamma_f,a;e_i}(E,p^0_i)-\frac{1}{2}\oint_\Gamma dE g^{(0)}_{\gamma_f,a;e_i}(E,p^0_i)\frac{1}{2\pi i}\oint_\Gamma dE g^{(1)}_a(E)$$

$$+(Z_2^{-1/2}-1)\oint_\Gamma dE g^{(0)}_{\gamma_f,a;e_i}(E,p^0_i)\Bigg], \tag{19}$$

where $g^{(1)}_a(E)$ is defined by the first-order self-energy diagram. We omitted here the factor $Z_3^{-1/2}$ in the last term since it contributes only to the vacuum-polarization (VP) correction. Consider first the diagram (a). According to the Feynman rules from Ref. [10], we have

$$G^{(1,a)}_{\gamma_f,e_i}(k^0,E,p^0,\mathbf{x}')=\delta(E+k^0-p^0)\int d\mathbf{x}d\mathbf{y}d\mathbf{z}\frac{i}{2\pi}S(E,\mathbf{x}',\mathbf{x})\frac{2\pi}{i}\gamma^0\Sigma(E,\mathbf{x},\mathbf{y})$$

$$\times\frac{i}{2\pi}S(E,\mathbf{y},\mathbf{z})A^*_{f,\nu}(\mathbf{z})(-ie\gamma^\nu 2\pi)\psi_{p_i\mu_i(+)}(\mathbf{z}), \tag{20}$$

where

$$\Sigma(E,\mathbf{x},\mathbf{y})=e^2\frac{i}{2\pi}\int d\omega\,\gamma^0\gamma^\rho S(E-\omega,\mathbf{x},\mathbf{y})\,\gamma^\sigma D_{\rho\sigma}(\omega,\mathbf{x}-\mathbf{y}) \tag{21}$$

is the self-energy operator,

$$D_{\rho\sigma}(\omega,\mathbf{x}-\mathbf{y})=-g_{\rho\sigma}\int\frac{d\mathbf{k}}{(2\pi)^3}\frac{\exp[i\mathbf{k}\cdot(\mathbf{x}-\mathbf{y})]}{\omega^2-\mathbf{k}^2-\mu^2+i0} \tag{22}$$

is the photon propagator in the Feynman gauge, and μ is a photon mass which is introduced to regularize the infrared divergences. According to the definition (6) one finds

$$g^{(1,a)}_{\gamma_f,a;e_i}(E,p^0)=\sum_n\frac{\langle a|\Sigma(E)|n\rangle\langle n|e\alpha^\nu A^*_{f,\nu}|p_i,\mu_i\rangle}{(E-\varepsilon_a)(E-\varepsilon_n)} \tag{23}$$

and

$$\oint_\Gamma dE\,g^{(1,a)}_{\gamma_f,a;e_i}(E,p_i^0)=2\pi i\left[\sum_{n\neq a}\frac{\langle a|\Sigma(\varepsilon_a)|n\rangle\langle n|e\alpha^\nu A^*_{f,\nu}|p_i,\mu_i\rangle}{\varepsilon_a-\varepsilon_n}+\langle a|\Sigma'(\varepsilon_a)|a\rangle\langle a|e\alpha^\nu A^*_{f,\nu}|p_i,\mu_i\rangle\right], \tag{24}$$

where $\Sigma'(\varepsilon_a)\equiv d\Sigma(\varepsilon)/d\varepsilon\big|_{\varepsilon=\varepsilon_a}$. A similar calculation of the diagrams (c) and (b) gives

$$\oint_\Gamma dE\,g^{(1,c)}_{\gamma_f,a;e_i}(E,p_i^0)=2\pi i\sum_n\frac{\langle a|e\alpha^\nu A^*_{f,\nu}|n\rangle\langle n|\Sigma(p_i^0)|p_i,\mu_i\rangle}{p_i^0-\varepsilon_n(1-i0)} \tag{25}$$

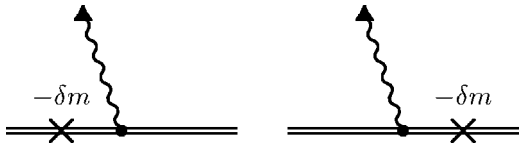

FIG. 3. The mass counterterm corrections to the radiative recombination of an electron with a bare nucleus.

and

$$\oint_\Gamma dE\,g^{(1,b)}_{\gamma_f,a;e_i}(E,p_i^0)=2\pi i\int d\mathbf{z}eA^*_{f,\nu}(\mathbf{z})\Lambda^\nu(\varepsilon_a,p_i^0,\mathbf{z}), \tag{26}$$

where

$$\Lambda^\nu(\varepsilon,p^0,\mathbf{z})=e^2\frac{i}{2\pi}\int_{-\infty}^{\infty}d\omega\int d\mathbf{x}d\mathbf{y}\,\overline{\psi_a}(\mathbf{x})\,\gamma^\rho S(\varepsilon-\omega,\mathbf{x},\mathbf{z})\times\gamma^\nu S(p^0-\omega,\mathbf{z},\mathbf{y})\,\gamma^\sigma D_{\rho\sigma}(\omega,\mathbf{x}-\mathbf{y})\times\psi_{p_i\mu_i(+)}(\mathbf{y}). \tag{27}$$

Let us now calculate the second term in Eq. (19). A simple calculation of the second factor in this term yields

$$\frac{1}{2\pi i}\oint_\Gamma dE\,g^{(1)}_a(E)=\langle a|\Sigma'(\varepsilon_a)|a\rangle. \tag{28}$$

We obtain

$$-\frac{1}{2}\oint_\Gamma dE\,g^{(0)}_{\gamma_f,a;e_i}(E,p_i^0)\frac{1}{2\pi i}\oint_\Gamma dE\,g^{(1)}_a(E)=-\frac{1}{2}2\pi i\langle a|e\alpha^\nu A^*_{f,\nu}|p_i,\mu_i\rangle\langle a|\Sigma'(\varepsilon_a)|a\rangle. \tag{29}$$

Substituting Eqs. (24)–(26), (29) into Eq. (19), taking into account Eq. (16), and adding the contribution of the mass-counterterm diagrams (Fig. 3), we find

$$\langle k_f,\epsilon_f;a|S^{(1)}_{\rm SE}|p_i,\mu_i\rangle=-2\pi i\,\delta(\varepsilon_a+k_f^0-p_i^0)\left[\sum_{n\neq a}\frac{\langle a|\Sigma(\varepsilon_a)-\beta\delta m|n\rangle\langle n|e\alpha^\nu A^*_{f,\nu}|p_i,\mu_i\rangle}{\varepsilon_a-\varepsilon_n}+\frac{1}{2}\langle a|\Sigma'(\varepsilon_a)|a\rangle\langle a|e\alpha^\nu A^*_{f,\nu}|p_i,\mu_i\rangle+\sum_n\frac{\langle a|e\alpha^\nu A^*_{f,\nu}|n\rangle\langle n|\Sigma(p_i^0)-\beta\delta m|p_i,\mu_i\rangle}{p_i^0-\varepsilon_n(1-i0)}+\int d\mathbf{z}eA^*_{f,\nu}(\mathbf{z})\Lambda^\nu(\varepsilon_a,p_i^0,\mathbf{z})+(Z_2^{-1/2}-1)\langle a|e\alpha^\nu A^*_{f,\nu}|p_i,\mu_i\rangle\right]. \tag{30}$$

A similar calculation of the VP corrections [Fig. 2, diagrams (d)–(f)] gives

$$\langle k_f,\epsilon_f;a|S^{(1)}_{\rm VP}|p_i,\mu_i\rangle=-2\pi i\,\delta(\varepsilon_a+k_f^0-p_i^0)\Bigg[\sum_{n\neq a}\frac{\langle a|U_{\rm VP}|n\rangle\langle n|e\alpha^\nu A^*_{f,\nu}|p_i,\mu_i\rangle}{\varepsilon_a-\varepsilon_n}$$
$$+\sum_n\frac{\langle a|e\alpha^\nu A^*_{f,\nu}|n\rangle\langle n|U_{\rm VP}|p_i,\mu_i\rangle}{p_i^0-\varepsilon_n(1-i0)}+\int d\mathbf{z}eA^*_{f,\nu}(\mathbf{z})Q^\nu(k_f^0,\mathbf{z})+(Z_3^{-1/2}-1)\langle a|e\alpha^\nu A^*_{f,\nu}|p_i,\mu_i\rangle\Bigg]. \tag{31}$$

Here

$$U_{\rm VP}(\mathbf{x})=\frac{\alpha}{2\pi i}\int d\mathbf{y}\frac{1}{|\mathbf{x}-\mathbf{y}|}\int_{-\infty}^{\infty}d\omega\,{\rm Tr}[S(\omega,\mathbf{y},\mathbf{y})\gamma^0] \tag{32}$$

is the VP potential and

$$Q^\nu(k^0,\mathbf{z})=-e^2\int d\mathbf{x}d\mathbf{y}\bar{\psi}_a(\mathbf{x})\gamma^\rho\psi_{p_i\mu_i(+)}(\mathbf{x})D_{\rho\sigma}(k^0,\mathbf{x}-\mathbf{y})$$
$$\times\frac{i}{2\pi}\int_{-\infty}^{\infty}d\omega\,{\rm Tr}[\gamma^\sigma S(\omega,\mathbf{y},\mathbf{z})\gamma^\nu S(\omega+k^0,\mathbf{z},\mathbf{y})]. \tag{33}$$

Comparing the expressions (30),(31) with the related expressions of Ref. [8] we find that the contribution of the reducible part of the diagram with the SE loop on the outgoing electron line [the second term in the right side of Eq. (30)] is absent in Ref. [8].

Some individual terms in Eqs. (30) and (31) contain ultraviolet divergences. These divergences arise solely from the zero- and one-potential terms in the expansion of the electron propagators in powers of the external potential. Using the standard expressions for the divergent parts of the zero- and one-potential SE terms (see, e.g., Ref. [11]) and the Ward identity ($Z_1=Z_2$) one easily finds that the ultraviolet divergences cancel each other in Eq. (30). As to Eq. (31), the divergent parts incorporate into the charge renormalization factor ($e=Z_3^{1/2}e_0$).

An alternative approach to the renormalization problem consists in using from the very beginning the renormalized field operators $\psi_R=Z_2^{-1/2}\psi$, $A_R=Z_3^{-1/2}A$, the renormalized electron charge $e=e_0+\delta e=Z_1^{-1}Z_2Z_3^{1/2}e_0$ and, respectively, the renormalized Green functions. As a result, the renormalization constants Z_2 and Z_3 disappear from the reduction formulas (3) and (4) and, instead, additional counterterms arise in the diagram technique rules.

In addition to the QED corrections derived in this section, we must take into account the contribution originating from changing the photon energy in the zeroth-order cross section (18) due to the QED correction to the energy of the bound state a. It follows that the total QED correction of first order in α to the cross section is given by

$$\frac{d\sigma^{(1)}_{\rm QED}}{d\Omega_f}=\frac{(2\pi)^4}{v_i}\mathbf{k}_f^2 2{\rm Re}\{\tau^{(0)*}\tau^{(1)}_{\rm QED}\}$$
$$+\left[\left.\frac{d\sigma^{(0)}}{d\Omega_f}\right|_{k_f^0=p_i^0-\varepsilon_a}-\left.\frac{d\sigma^{(0)}}{d\Omega_f}\right|_{k_f^0=p_i^0-\varepsilon_a^{(0)}}\right]. \tag{34}$$

Here $\tau^{(1)}_{\rm QED}=\tau^{(1)}_{\rm SE}+\tau^{(1)}_{\rm VP}$ is the QED correction given by Eqs. (30) and (31) in accordance with the definition (2). ε_a and $\varepsilon_a^{(0)}$ are the energies of the bound state a with and without the QED correction, respectively.

V. INFRARED DIVERGENCES

Let us now consider the infrared divergent part of τ. This part results from the region of small momenta of the virtual photon and is regularized by the nonzero photon mass μ. The first term in the right side of Eq. (30) does not contain infrared divergences. A simple evaluation of the infrared divergent parts of the second, third, and fifth terms yields

$$\frac{1}{2}[\langle a|\Sigma'(\varepsilon_a)|a\rangle\langle a|e\alpha^\nu A^*_{f,\nu}|p_i,\mu_i\rangle]_{\rm infr}$$
$$=\frac{1}{2}[Z_2-1]_{\rm infr}\langle a|e\alpha^\nu A^*_{f,\nu}|p_i,\mu_i\rangle, \tag{35}$$

$$\left[\sum_n\frac{\langle a|e\alpha^\nu A^*_{f,\nu}|n\rangle\langle n|\Sigma(p_i^0)-\beta\delta m|p_i,\mu_i\rangle}{p_i^0-\varepsilon_n(1-i0)}\right]_{\rm infr}$$
$$=[Z_2-1]_{\rm infr}\langle a|e\alpha^\nu A^*_{f,\nu}|p_i,\mu_i\rangle, \tag{36}$$

$$[(Z_2^{-1/2}-1)\langle a|e\alpha^\nu A^*_{f,\nu}|p_i,\mu_i\rangle]_{\rm infr}$$
$$=-\frac{1}{2}[Z_2-1]_{\rm infr}\langle a|e\alpha^\nu A^*_{f,\nu}|p_i,\mu_i\rangle. \tag{37}$$

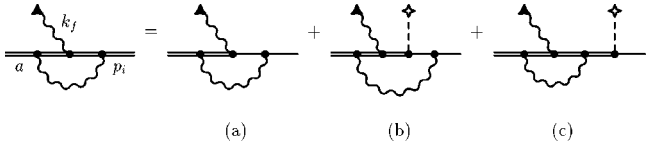

FIG. 4. Decomposition of the vertex diagram in powers of the Coulomb field. The single line denotes a free electron and the double line denotes an electron propagating in the Coulomb field.

Summing these terms we find in the Feynman gauge

$$[Z_2-1]_{\rm infr}\langle a|e\alpha^\nu A^*_{f,\nu}|p_i,\mu_i\rangle=-\frac{\alpha}{\pi}\ln(\mu/m)\times\langle a|e\alpha^\nu A^*_{f,\nu}|p_i,\mu_i\rangle, \tag{38}$$

To derive the infrared divergent part of the fourth term in Eq. (30), we expand the vertex diagram in powers of the Coulomb field as shown in Fig. 4. In this figure the single line indicates the free electron and the double line indicates the electron propagating in the Coulomb field of the nucleus. The dashed line ended by the cross denotes the interaction with the Coulomb field. The infrared divergences arise only from the diagrams (a) and (b). The contribution of the diagram (a) is

$$\tau^{(a)}=-e^2\frac{i}{2\pi}\int_{-\infty}^{\infty}d\omega\int d\mathbf{x}d\mathbf{y}d\mathbf{z}\overline{\psi}_a(\mathbf{x})\gamma^\rho\sum_n\frac{\psi_n(\mathbf{x})\overline{\psi}_n(\mathbf{z})}{\varepsilon_a-\omega-\varepsilon_n(1-i0)}\gamma^\nu eA^*_{f,\nu}(\mathbf{z})$$
$$\times\sum_\lambda\int d\mathbf{q}\left(\frac{U_{q\lambda}(\mathbf{z})\overline{U}_{q\lambda}(\mathbf{y})}{p_i^0-\omega-\sqrt{\mathbf{q}^2+m^2}+i0}-\frac{V_{q\lambda}(\mathbf{z})\overline{V}_{q\lambda}(\mathbf{y})}{p_i^0-\omega+\sqrt{\mathbf{q}^2+m^2}-i0}\right)$$
$$\times\gamma^\sigma(-g_{\rho\sigma})\int\frac{d\mathbf{k}}{(2\pi)^3}\frac{\exp(i\mathbf{k}\cdot(\mathbf{x}-\mathbf{y}))}{\omega^2-\mathbf{k}^2-\mu^2+i0}U_{p_i\mu_i}(\mathbf{y}), \tag{39}$$

where

$$U_{q\lambda}(\mathbf{x})=\frac{u(q,\lambda)\exp(i\mathbf{q}\cdot\mathbf{x})}{\sqrt{\frac{q^0}{m}(2\pi)^3}},$$

$$V_{q\lambda}(\mathbf{x})=\frac{v(q,\lambda)\exp(-i\mathbf{q}\cdot\mathbf{x})}{\sqrt{\frac{q^0}{m}(2\pi)^3}},$$

$u(q,\lambda)$ and $v(q,\lambda)$ are the Dirac bispinors corresponding to the positive and negative energy states, respectively. They are normalized by the equations

$$\overline{u}(q,\lambda)u(q,\lambda')=\delta_{\lambda\lambda'},\quad \overline{v}(q,\lambda)v(q,\lambda')=-\delta_{\lambda\lambda'},$$

$$\overline{v}(q,\lambda)u(q,\lambda')=0.$$

The infrared singularity in Eq. (39) results from the region of small momenta in the integration over $\mathbf{k}$. Only the term with $n=a$ and the positive energy part of the free electron propagator contribute to this singularity. Taking into account that for small $\mathbf{k}$

$$\int d\mathbf{x}U^\dagger_{q\lambda}(\mathbf{x})\exp(-i\mathbf{k}\cdot\mathbf{x})U_{p_i\mu_i}(\mathbf{x})\approx\delta(\mathbf{q}+\mathbf{k}-\mathbf{p}_i)\delta_{\lambda\mu_i}$$

and

$$\int d\mathbf{x}\psi^\dagger_a(\mathbf{x})\exp(i\mathbf{k}\cdot\mathbf{x})\psi_a(\mathbf{x})\approx\int d\mathbf{x}\psi^\dagger_a(\mathbf{x})\psi_a(\mathbf{x})=1,$$

we obtain for the infrared part

$$\tau^{(a)}_{\rm infr}=e^2\frac{i}{2\pi}\int_{-\infty}^{\infty}d\omega\frac{1}{-\omega+i0}\int_{|\mathbf{k}|\ll m}\frac{d\mathbf{k}}{(2\pi)^3}\int d\mathbf{x}\overline{\psi}_a(\mathbf{x})e\gamma^\nu A^*_{f,\nu}(\mathbf{x})U_{p_i\mu_i}(\mathbf{x})\frac{1}{\omega^2-\mathbf{k}^2-\mu^2+i0}\frac{1}{p_i^0-\omega-\sqrt{(\mathbf{p}_i-\mathbf{k})^2+m^2}+i0}$$
$$=-e^2\int d\mathbf{x}\overline{\psi}_a(\mathbf{x})e\gamma^\nu A^*_{f,\nu}(\mathbf{x})U_{p_i\mu_i}(\mathbf{x})\int_{|\mathbf{k}|\ll m}\frac{d\mathbf{k}}{(2\pi)^3}\frac{1}{2(\mathbf{k}^2+\mu^2)(p_i^0-\sqrt{\mathbf{k}^2+\mu^2}-\sqrt{(\mathbf{p}_i-\mathbf{k})^2+m^2})}. \tag{40}$$

Integrating over $\mathbf{k}$ and retaining only the terms which are singular at $\mu\to0$ we obtain

$$\tau^{(a)}_{\rm infr}=-\int d\mathbf{x}\bar{\psi}_a(\mathbf{x})e\gamma^\nu A^*_{f,\nu}(\mathbf{x})U_{p_i\mu_i}(\mathbf{x})\frac{\alpha}{2\pi}\log(m/\mu)\sqrt{1+\frac{m^2}{\mathbf{p}_i^2}}\ln\left(\frac{\sqrt{\mathbf{p}_i^2+m^2}-|\mathbf{p}_i|}{\sqrt{\mathbf{p}_i^2+m^2}+|\mathbf{p}_i|}\right). \tag{41}$$

A similar evaluation of the diagram (b) and adding it to Eq. (41) results in replacement of $U_{p_i\mu_i}(\mathbf{x})$ in Eq. (41) by $\psi_{p_i\mu_i(+)}(\mathbf{x})$ defined by Eq. (14). So, we have

$$\tau^{(a+b)}_{\rm infr}=\tau^{(0)}\frac{\alpha}{2\pi}\ln(m/\mu)\sqrt{1+\frac{m^2}{\mathbf{p}_i^2}}\ln\left(\frac{\sqrt{\mathbf{p}_i^2+m^2}-|\mathbf{p}_i|}{\sqrt{\mathbf{p}_i^2+m^2}+|\mathbf{p}_i|}\right), \tag{42}$$

where τ_0 is the zeroth-order contribution given by Eq. (17). Summing this term with the infrared contribution from the other terms, given by Eq. (38), we find

$$\tau_{\rm infr}=\tau^{(0)}\frac{\alpha}{\pi}\left[-\ln(\mu/m)-\frac{1}{2}\ln(\mu/m)\sqrt{1+\frac{m^2}{\mathbf{p}_i^2}}\times\ln\left(\frac{\sqrt{\mathbf{p}_i^2+m^2}-|\mathbf{p}_i|}{\sqrt{\mathbf{p}_i^2+m^2}+|\mathbf{p}_i|}\right)\right]. \tag{43}$$

The related contribution to the cross section according to Eq. (1) is

$$\frac{d\sigma_{\rm infr}}{d\Omega_f}=\frac{d\sigma^{(0)}}{d\Omega_f}\frac{\alpha}{\pi}\left[-2\ln(\mu/m)-\ln(\mu/m)\sqrt{1+\frac{m^2}{\mathbf{p}_i^2}}\times\log\left(\frac{\sqrt{\mathbf{p}_i^2+m^2}-|\mathbf{p}_i|}{\sqrt{\mathbf{p}_i^2+m^2}+|\mathbf{p}_i|}\right)\right], \tag{44}$$

where $d\sigma^{(0)}/d\Omega_f$ is the cross section in the zeroth-order approximation defined by Eq. (18).

As is known (see, e.g., Ref. [12,13]), to cancel the infrared divergent contribution (44) we must take into account that any experiment has a finite energy resolution ΔE. It means that any numbers of photons of the total energy less than ΔE can be emitted in the process. It follows that to find the total cross section in the order under consideration we must include diagrams in which one photon of energy $k^0=\sqrt{\mathbf{k}^2+\mu^2}$ less than ΔE is emitted along with the emission of the photon with the energy $k_f^0\approx p_i^0-\varepsilon_a$ (we assume $\Delta E\ll k_f^0$). These diagrams are shown in Fig. 5. Assuming that the energy resolution is high enough ($\Delta E\ll k_f^0,m$) we will retain only those contributions from the diagrams shown in Fig. 5 which dominate at $\Delta E\to 0$. These contributions result just from the infrared divergent parts of the diagrams. The infrared divergent terms are defined by the diagrams depicted in Fig. 6. Using the standard technique described, e.g., in Ref. [12] one can find that the infrared divergent part of the diagrams shown in Fig. 6 is

$$\tau^{(a)}_{\gamma,\rm infr}=\tau^{(0)}\frac{e\boldsymbol{\epsilon}\cdot p_i}{p_i^0-\sqrt{\mathbf{k}^2+\mu^2}-\sqrt{(\mathbf{p}_i-\mathbf{k})^2+m^2}}\frac{1}{p_i^0\sqrt{2k^0(2\pi)^3}}, \tag{45}$$

where $\tau^{(0)}$ is given by Eq. (17), $\mathbf{k}$ is the momentum of the soft photon and $\boldsymbol{\epsilon}$ is its polarization. To find the related contribution to the cross section we must evaluate

$$\frac{d\sigma_\gamma(\Delta E)}{d\Omega_f}=\frac{(2\pi)^4}{v_i}\mathbf{k}_f^2\sum_\lambda\int_{|\mathbf{k}|\le\Delta E}d\mathbf{k}|\tau_\gamma|^2, \tag{46}$$

where the index λ runs over the polarizations of the soft photon. Using the identity [12]

$$\sum_\lambda(\boldsymbol{\epsilon}\cdot p)(\boldsymbol{\epsilon}\cdot p)=\mathbf{p}^2-\frac{(\mathbf{p}\cdot\mathbf{k})^2}{(k^0)^2} \tag{47}$$

we find

$$\sum_\lambda\int_{|\mathbf{k}|\le\Delta E}d\mathbf{k}|\tau_\gamma|^2=|\tau^{(0)}|^2e^2\int_{|\mathbf{k}|\le\Delta E}\frac{d\mathbf{k}}{(2\pi)^3}\frac{(\mathbf{k}^2+\mu^2)\mathbf{p}_i^2-(\mathbf{p}_i\cdot\mathbf{k})^2}{2(\mathbf{k}^2+\mu^2)^{3/2}(p_i^0)^2}\times\frac{1}{(p_i^0-\sqrt{\mathbf{k}^2+\mu^2}-\sqrt{(\mathbf{p}_i-\mathbf{k})^2+m^2})^2}. \tag{48}$$

Integrating over $\mathbf{k}$ in Eq. (48) and omitting terms which approach zero at $\mu\to 0$, we obtain

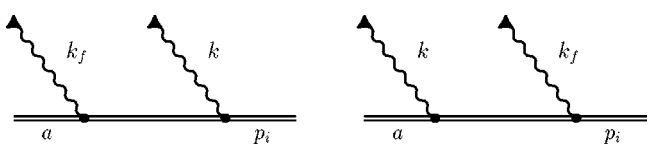

FIG. 5. The radiative recombination accompanied by emission of a soft photon.

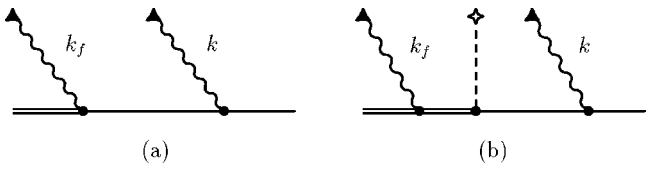

FIG. 6. The infrared divergent part of the radiative recombination accompanied by emission of a soft photon.

$$\frac{d\sigma_\gamma(\Delta E)}{d\Omega_f}=\frac{d\sigma^{(0)}}{d\Omega_f}\frac{\alpha}{\pi}\Bigg[1-2\ln 2-2\log(\Delta E/\mu)-\sqrt{1+\frac{m^2}{\mathbf{p}_i^2}}F(|\mathbf{p}_i|/p_i^0)-\left(\frac{1}{2}+\ln(\Delta E/\mu)\right)\times\sqrt{1+\frac{m^2}{\mathbf{p}_i^2}}\ln\left(\frac{\sqrt{\mathbf{p}_i^2+m^2}-|\mathbf{p}_i|}{\sqrt{\mathbf{p}_i^2+m^2}+|\mathbf{p}_i|}\right)\Bigg], \tag{49}$$

where

$$F(a)=\int_0^\infty dx\,\frac{x}{x^2+1}\ln\left[\frac{(1+a)(\sqrt{x^2+1}-ax)}{(1-a)(\sqrt{x^2+1}+ax)}\right]. \tag{50}$$

One can see that the infrared divergent parts in Eqs. (44) and (49) cancel each other:

$$\frac{d\sigma_{\rm infr}}{d\Omega_f}+\frac{d\sigma_\gamma(\Delta E)}{d\Omega_f}=\frac{d\sigma^{(0)}}{d\Omega_f}\frac{\alpha}{\pi}\Bigg[1-2\ln 2-2\ln(\Delta E/m)-\sqrt{1+\frac{m^2}{\mathbf{p}_i^2}}F(|\mathbf{p}_i|/p_i^0)-\left(\frac{1}{2}+\ln(\Delta E/m)\right)\sqrt{1+\frac{m^2}{\mathbf{p}_i^2}}\times\ln\left(\frac{\sqrt{\mathbf{p}_i^2+m^2}-|\mathbf{p}_i|}{\sqrt{\mathbf{p}_i^2+m^2}+|\mathbf{p}_i|}\right)\Bigg]. \tag{51}$$

According to this equation, at a fixed energy of the incident electron the QED correction depends on the photon-energy resolution ΔE and becomes infinite when $\Delta E\to 0$. It means that the validity of this equation is restricted by the condition $(\alpha/\pi)|\log(\Delta E/m)|\ll 1$. For extension of the theory beyond this limit it is necessary to include the radiative corrections of higher orders in α (see Refs. [12,13], and references therein). It results in an ''exponentiation'' of the radiative corrections and removes the singularity for $\Delta E\to 0$.

VI. ELECTRON ENERGY DISTRIBUTION

In the derivation of the formulas (49),(51) we assumed that the incident electrons have a fixed energy. These formulas remain also valid in the case when the energy spread of the incident electrons is much smaller than the energy interval ΔE in which the photons are detected. Let us now consider how we should modify the formulas to calculate the QED corrections to the RR cross section if the energy spread of the incident electrons characterized by a parameter Γ is much larger than ΔE. For simplicity, we will neglect the transverse component of the electron momentum. Let us represent the energy of an incident electron as $\varepsilon=\varepsilon_a+k_f^0+x$. Only if $x>0$, the electron can be captured to the state a with the emission of a photon in the energy interval $(k_f^0,k_f^0+\Delta E)$. For $\Delta E>x>0$ the cross section of this process is equal to the cross section with the electron energy $\varepsilon=\varepsilon_a+k_f^0+x$ and with x considered as the upper limit for the soft photon energy. For $x>\Delta E$ the cross section under consideration is the difference of the related cross sections with the soft-photon-energy limits x and $x-\Delta E$, respectively. If the energy distribution of the incident electrons is described by a function $f(\varepsilon)$, the total cross section into the interval of the photon energy $(k_f^0,k_f^0+\Delta E)$ is

$$\begin{aligned}\frac{d\overline{\sigma}(\Delta E)}{d\Omega_f}&=\int_0^{\Delta E}dx f(\varepsilon_a+k_f^0+x)\frac{d\sigma(x)}{d\Omega_f}+\int_{\Delta E}^\infty dx f(\varepsilon_a+k_f^0+x)\left[\frac{d\sigma(x)}{d\Omega_f}-\frac{d\sigma(x-\Delta E)}{d\Omega_f}\right]\\&=\int_0^\infty dx f(\varepsilon_a+k_f^0+x)\frac{d\sigma(x)}{d\Omega_f}-\int_{\Delta E}^\infty dx f(\varepsilon_a+k_f^0+x)\frac{d\sigma(x-\Delta E)}{d\Omega_f},\end{aligned} \tag{52}$$

where $d\sigma(x)/d\Omega_f$ and $d\sigma(x-\Delta E)/d\Omega_f$ are the cross sections with the electron energy $\varepsilon_a+k_f^0+x$ and with the soft-photon-energy limits x and $x-\Delta E$, respectively. Assuming a very weak dependence of $d\sigma(x)/d\Omega_f$ on the electron energy within the electron energy spread interval and taking into account that $\Delta E\ll\Gamma$ we obtain

$$\begin{aligned}\frac{1}{\Delta E}\frac{d\overline{\sigma}(\Delta E)}{d\Omega_f}&\approx\int_0^\infty dx\frac{d\sigma(x)}{d\Omega_f}\frac{[f(\varepsilon_a+k_f^0+x)-f(\varepsilon_a+k_f^0+x+\Delta E)]}{\Delta E}\\&\approx-\int_0^\infty dx\frac{d\sigma(x)}{d\Omega_f}\frac{df(\varepsilon_a+k_f^0+x)}{dx}.\end{aligned} \tag{53}$$

According to Eq. (51), the cross section $d\sigma(x)/d\Omega_f$ including the lowest order QED corrections can be written as

$$\frac{d\sigma(x)}{d\Omega_f}=A\ln x+B. \tag{54}$$

It follows that for any reasonable function $f(\varepsilon)$ the integral in Eq. (53) is convergent at small x and

$$(1/\Delta E)[d\overline{\sigma}(\Delta E)/d\Omega_f]$$

does not depend on ΔE. If we assume, for instance, a Lorentz-type form for $f(\varepsilon)$,

$$f(\varepsilon)=\frac{1}{2\pi}\frac{\Gamma}{(\varepsilon-\varepsilon_0)^2+\frac{\Gamma^2}{4}}, \tag{55}$$

integrating over x in Eq. (53) yields

$$\frac{1}{\Delta E}\frac{d\bar{\sigma}(\Delta E)}{d\Omega_f}=\frac{1}{2\pi}\frac{\Gamma}{(\varepsilon_a+k_f^0-\varepsilon_0)^2+\frac{\Gamma^2}{4}}\times\left\{B+A\left[\frac{1}{2}\ln[(\varepsilon_a+k_f^0-\varepsilon_0)^2+(\Gamma^2/4)]-\frac{\varepsilon_a+k_f^0-\varepsilon_0}{\Gamma}\times\{\pi-2\arctan[2(\varepsilon_a+k_f^0-\varepsilon_0)/\Gamma]\}\right]\right\}. \tag{56}$$

For a rectangular form for $f(\varepsilon)$,

$$f(\varepsilon)=\frac{1}{\Gamma}\theta(\varepsilon-\varepsilon_0+\Gamma/2)\,\theta(\varepsilon_0+\Gamma/2-\varepsilon), \tag{57}$$

where $\theta(x)=(x+|x|)/(2|x|)$, one finds

$$\frac{1}{\Delta E}\frac{d\bar{\sigma}(\Delta E)}{d\Omega_f}=\frac{1}{\Gamma}\frac{d\sigma(\varepsilon_0+\Gamma/2-\varepsilon_a-k_f^0)}{d\Omega_f} \tag{58}$$

if $\varepsilon_a+k_f^0$ belongs to the interval $(\varepsilon_0-\Gamma/2,\varepsilon_0+\Gamma/2)$. As one can see from Eqs. (56),(58), for $\Delta E\ll\Gamma$ the cross section depends on Γ but not on ΔE.

In the REC experiments [1,2] the effective energy spread caused by the momentum spread of a quasifree target electron bound in a low-Z target atom is much larger than the photon-energy resolution. It follows that the formula (51) cannot be directly employed for the calculation of the QED corrections to the REC cross section into the photon-energy interval determined by the photon-energy resolution. However, it can be used for the evaluation of the QED corrections to the REC cross section into a photon-energy interval ΔE $(\Delta E\ll k_f^0,m)$ which is much larger than the effective energy spread of the target electron.

VII. NUMERICAL RESULTS

As is known from calculations of QED effects for bound states (see [7] and references therein), the dominant contribution of the vacuum polarization correction can be obtained by using the Uehling approximation. In this approximation the vacuum polarization potential in the diagrams depicted in Figs. 2(d),2(f) is replaced by the Uehling potential which is the first nonvanishing term in the decomposition of the vacuum loop in powers of the external Coulomb field. As to the diagram depicted in Fig. 2(e), one can show that it does not contribute in the Uehling approximation.

In Refs. [14,15] we evaluated numerically the Uehling part of the VP correction to the RR cross section by including the Uehling potential into the Dirac equation and taking the difference between the cross section obtained with the modified wave functions and bound-state energy and the cross section obtained with the unperturbed wave functions and bound-state energy. In this method, in addition to the Uehling correction of the first order in α, higher-order iterations of the Uehling potential are accounted for as well. Since the higher-order corrections decrease rapidly with increasing number of the VP loops, this approach serves as a good estimation scheme for the Uehling correction of the first order in α.

TABLE I. The relative values of the QED corrections to the total cross section for the radiative recombination into the K shell of bare uranium, expressed in percent.

Impact energy	Correction	Vacuum polarization, in %	Self-energy, in %
100 MeV/u	$\sigma_{\rm en}^{(1)}$	0.061	−0.230
	$\sigma_{\rm bw}^{(1)}$	0.065	−0.160
	$\sigma_{\rm cw}^{(1)}$	−0.006	?
	Total	0.120	−0.390
300 MeV/u	$\sigma_{\rm en}^{(1)}$	0.058	−0.219
	$\sigma_{\rm bw}^{(1)}$	0.117	−0.295
	$\sigma_{\rm cw}^{(1)}$	−0.003	?
	Total	0.173	−0.513
1000 MeV/u	$\sigma_{\rm en}^{(1)}$	0.056	−0.211
	$\sigma_{\rm bw}^{(1)}$	0.164	−0.380
	$\sigma_{\rm cw}^{(1)}$	0.043	?
	Total	0.263	−0.591

In the present work, the Uehling correction to the RR cross section is evaluated numerically according to the formula (34). The results of this evalution are in a good agreement with those from Refs. [14,15]. Expressed in terms of the unperturbed cross section, the individual Uehling corrections to the total cross section for the radiative recombination into the K shell of bare uranium are presented in the third column of Table I. This table contains also the numerical values for some SE corrections calculated in this work. The correction $\sigma_{\rm en}^{(1)}$ results from changing the bound state energy. It is determined by the term in the square brackets of Eq. (34). The correction $\sigma_{\rm bw}^{(1)}$ corresponds to the irreducible part of the diagrams describing the first-order QED effect on the bound-state electron wave function [Figs. 2(a),2(d)]. The correction $\sigma_{\rm cw}^{(1)}$ results from the diagrams describing the QED effect on the continuum-state wave function [Fig. 2(c), 2(f)]. The calculations of the QED corrections were performed by employing the methods developed in Refs. [16–18].

As in the bound-state QED, one may expect that the Uehling approximation accounts for a dominant part of the VP correction. As to the self-energy correction, we expect only that the terms calculated in this work give a reasonable estimate of the order of magnitude of the self energy correction which is beyond the correction depending on the photon-energy interval ΔE [see Eq. (51)]. The relative value of the last correction, which we denote by $\delta(\Delta E)$, is defined by

$$\delta(\Delta E)=\frac{\alpha}{\pi}\left[-2+\frac{1}{\beta}\ln\frac{1+\beta}{1-\beta}\right]\ln\frac{\Delta E}{m}, \tag{59}$$

where $\beta=v_i/c$. As it follows from the derivation of Eq. (51) and from the discussion in the previous section, the photon-

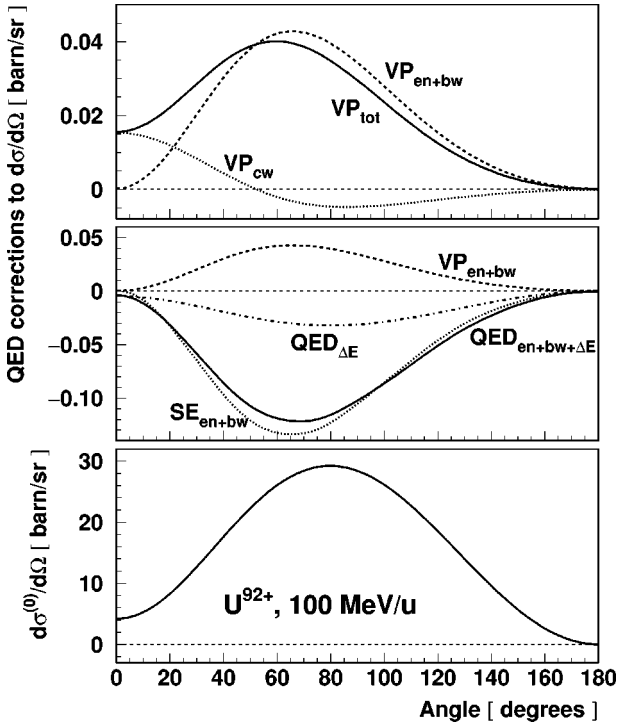

FIG. 7. The QED corrections to the differential cross section for the radiative recombination into the K shell of bare uranium at a projectile energy of 100 MeV/u, in the laboratory system. $\mathrm{VP}_{\mathrm{en+bw}}$ is the correction resulting from changing the bound-state energy and the bound-state wave function due to the vacuum polarization effect. $\mathrm{SE}_{\mathrm{en+bw}}$ denotes the corresponding self-energy correction. $\mathrm{VP}_{\mathrm{cw}}$ is the correction which accounts for the vacuum polarization effect on the continuum-state wave function. $\mathrm{VP}_{\mathrm{tot}}$ is the total vacuum polarization correction calculated in the Uehling approximation. $\mathrm{QED}_{\Delta E}$ denotes the correction which depends on the photon-energy interval. The relative value of this correction is defined by Eq. (59). The photon-energy interval is chosen to be 15 keV in the projectile frame. Since the correction due to the SE effect on the continuum-state wave function has not yet been calculated, the related VP correction is not included in the sum of the QED corrections denoted as $\mathrm{QED}_{\mathrm{en+bw+}\Delta E}$. $d\sigma^{(0)}/d\Omega$ is the zeroth-order cross section which is presented to display the relative values of the QED corrections.

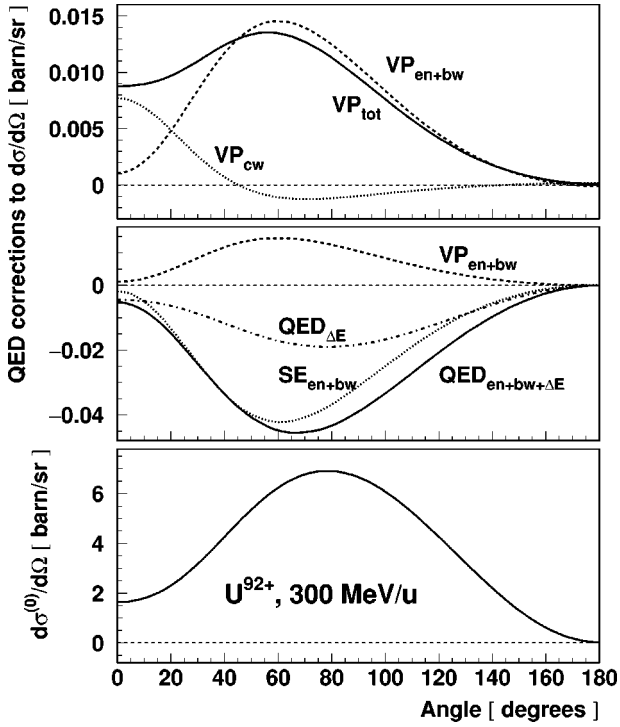

FIG. 8. The QED corrections to the differential cross section for the radiative recombination into the K shell of bare uranium at a projectile energy of 300 MeV/u, in the laboratory system. $\mathrm{VP}_{\mathrm{en+bw}}$ is the correction resulting from changing the bound-state energy and the bound-state wave function due to the vacuum polarization effect. $\mathrm{SE}_{\mathrm{en+bw}}$ denotes the corresponding self-energy correction. $\mathrm{VP}_{\mathrm{cw}}$ is the correction which accounts for the vacuum polarization effect on the continuum-state wave function. $\mathrm{VP}_{\mathrm{tot}}$ is the total vacuum polarization correction calculated in the Uehling approximation. $\mathrm{QED}_{\Delta E}$ denotes the correction which depends on the photon-energy interval. The relative value of this correction is defined by Eq. (59). The photon-energy interval is chosen to be 25 keV in the projectile frame. Since the correction due to the SE effect on the continuum-state wave function has not yet been calculated, the related VP correction is not included in the sum of the QED corrections denoted as $\mathrm{QED}_{\mathrm{en+bw+}\Delta E}$. $d\sigma^{(0)}/d\Omega$ is the zeroth-order cross section which is presented to display the relative values of the QED corrections.

energy interval has to be chosen in the range: $\Gamma \ll \Delta E \ll k_f^0, m$ where Γ characterizes the energy spread of the incident electrons. In the REC experiments which are being performed at GSI [1,2] the effective electron-energy spread is determined by the momentum distribution of the quasifree target electrons. The width of this spread in the projectile system increases with increasing the impact energy. In the case of a N_2 gas target, which is presently being employed in the experiments, the effective energy spread in the projectile (heavy ion) frame amounts to about 10–40 keV for the impact energy in the range 100–1000 MeV/u. This value will be considerably reduced in the experiments on a H_2 gas target which are under preparation. In the case of a H_2 gas target, to satisfy the conditions on ΔE given above we can choose ΔE to be 15, 25, and 50 keV in the projectile frame for the impact energies 100, 300 MeV/u, and 1 GeV/u, respectively. The corresponding photon-energy intervals in the laboratory (gas-target) frame are determined according to the Lorentz transformation

$$\Delta E_{\mathrm{proj}} = \Delta E_{\mathrm{lab}} \gamma (1 - \beta \cos \theta_{\mathrm{lab}}), \tag{60}$$

where $\gamma = 1/\sqrt{1-\beta^2}$. At a fixed ΔE_{proj}, from this equation one finds ΔE_{lab} as a function of the polar angle. For the photon-energy intervals chosen above $\delta(\Delta E)$ amounts to -0.11, -0.28, and -0.59 % for the impact energy 100, 300 MeV/u, and 1 GeV/u, respectively. To find the complete self-energy correction, accurate calculations of the diagrams depicted in Figs. 2(b),2(c) are required.

Adding the Uehling correction and the part of the SE correction presented in Table I to the correction $\delta(\Delta E)$ evaluated above, we find the QED correction to the total cross section amounts to -0.38, -0.62, and -0.92 % for the

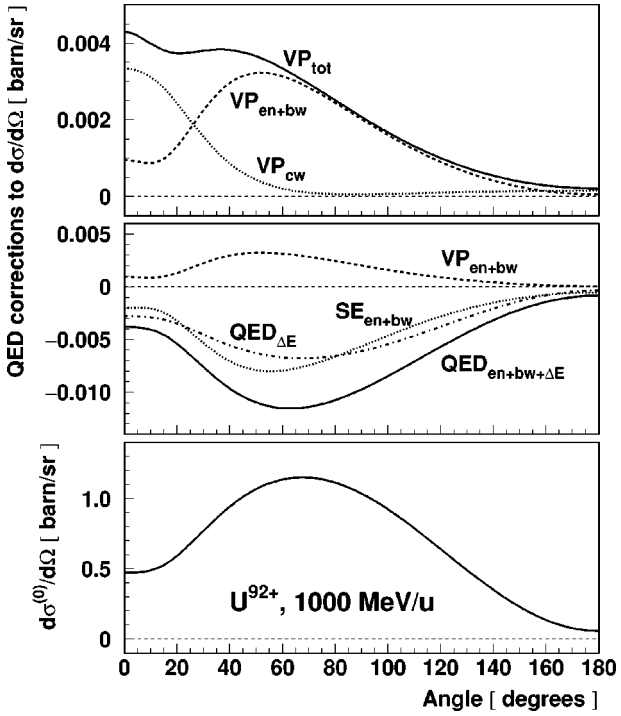

FIG. 9. The QED corrections to the differential cross section for the radiative recombination into the K shell of bare uranium at a projectile energy of 1000 MeV/u, in the laboratory system. $\mathrm{VP}_{\mathrm{en+bw}}$ is the correction resulting from changing the bound-state energy and the bound-state wave function due to the vacuum polarization effect. $\mathrm{SE}_{\mathrm{en+bw}}$ denotes the corresponding self-energy correction. $\mathrm{VP}_{\mathrm{cw}}$ is the correction which accounts for the vacuum polarization effect on the continuum-state wave function. $\mathrm{VP}_{\mathrm{tot}}$ is the total vacuum polarization correction calculated in the Uehling approximation. $\mathrm{QED}_{\Delta E}$ denotes the correction which depends on the photon-energy interval. The relative value of this correction is defined by Eq. (59). The photon-energy interval is chosen to be 50 keV in the projectile frame. Since the correction due to the SE effect on the continuum-state wave function has not yet been calculated, the related VP correction is not included in the sum of the QED corrections denoted as $\mathrm{QED}_{\mathrm{en+bw}+\Delta E}$. $d\sigma^{(0)}/d\Omega$ is the zeroth-order cross section which is presented to display the relative values of the QED corrections.

impact energy 100, 300 MeV/u, and 1 GeV/u, respectively. For comparison, the calculation of Ref. [9] gives -0.03, -0.13, and $-0.34\,\%$, respectively, for the same values of the photon-energy interval ΔE.

Figures 7, 8, and 9 show the angular dependence of the QED corrections to the radiative recombination into the K shell of bare uranium in the laboratory (gas-target) system. The transformation of the differential cross section from the projectile system to the laboratory system was done according to the formulas from Ref. [4]. In these figures, $\mathrm{VP}_{\mathrm{en+bw}}$ is the correction resulting from changing the bound-state energy and the bound-state wave function due to the vacuum polarization effect. $\mathrm{SE}_{\mathrm{en+bw}}$ denotes the corresponding self energy correction. $\mathrm{VP}_{\mathrm{cw}}$ is the correction which accounts for the vacuum polarization effect on the continuum-state wave function. $\mathrm{VP}_{\mathrm{tot}}$ is the total vacuum polarization correction calculated in the Uehling approximation. $\mathrm{QED}_{\Delta E}$ denotes the

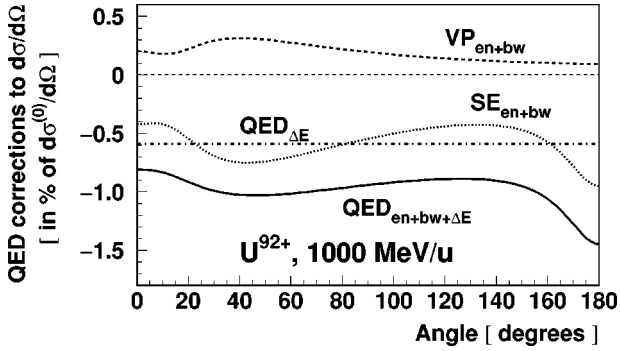

FIG. 10. The QED corrections to the differential cross section for the radiative recombination into the K shell of bare uranium at a projectile energy of 1000 MeV/u, expressed in percents of the zeroth-order cross section. For an explanation of the notations, see Fig. 9.

correction which depends on the photon-energy interval. The relative value of this correction, which is defined by Eq. (59), does not depend on the angles in both projectile and laboratory systems, if the photon-energy interval in the laboratory frame is chosen according to Eq. (60). Comparing the $\mathrm{VP}_{\mathrm{en+bw}}$ correction with the $\mathrm{SE}_{\mathrm{en+bw}}$ correction reveals a tendency of cancellation between them. Expecting a similar cancellation between the $\mathrm{VP}_{\mathrm{cw}}$ and $\mathrm{SE}_{\mathrm{cw}}$ contributions, we have not included the $\mathrm{VP}_{\mathrm{cw}}$ term into the sum of the QED corrections denoted as $\mathrm{QED}_{\mathrm{en+bw}+\Delta E}$. In order to display the relative values of the QED corrections, we present the zeroth-order cross section as well.

To present the relative magnitude of the calculated effects more clearly, the ratio of the QED corrections and the zeroth-order cross section is given in Fig. 10 for a projectile energy of 1 GeV/u. As one can see from this figure, the relative value of the $\mathrm{QED}_{\mathrm{en+bw}+\Delta E}$ correction varies from -0.8 % at the forward angles to -1.4% at the backward angles. However, the contribution of the QED corrections which are omitted in Fig. 10 may significantly change this behavior, especially at forward and backward angles.

It is also interesting to note that the differential cross section at the backward direction vanishes at an impact energy close to 130 MeV/u. It results, in particular, in relatively large contribution of the QED correction to the backward cross section at the energy 130 MeV/u. So, at this energy, the $\mathrm{QED}_{\mathrm{en+bw}+\Delta E}$ correction is about 0.022 mb/sr while the zeroth-order cross section amounts only to 0.009 mb/sr.

VIII. CONCLUSION

In this paper we derived the complete formulas for the QED corrections of the first order in α to the cross section of the radiative recombination of an electron with a bare nucleus. We found that, in addition to the expressions derived previously in Ref. [8], there is a nonzero contribution from the reducible part of the diagram with the self-energy loop on the outgoing electron line. The ultraviolet and infrared divergences of the QED corrections have been analyzed. In particular, we demonstrated that at a fixed incident electron energy the infrared divergence is eliminated in the total

cross section by allowing for the emission of an unobserved soft photon with an energy less than the photon-energy resolution. We note that the contribution of soft photons to the cross section depends on the energy interval in which the photons are detected if this interval is much larger than the effective energy spread of the incident electrons. If this interval is much smaller than the effective electron-energy spread, the contribution of soft photons is essentially determined by the parameters which define the line shape of the effective energy spread of the incident electrons. It does not depend on the energy resolution of the photon detector, provided this resolution is good enough to accurately define the line shape.

We evaluated numerically the Uehling part of the vacuum-polarization correction to the RR cross section and a part of the self-energy correction. The calculation of the total self-energy correction is under way and will be published elsewhere.

ACKNOWLEDGMENTS

We want to thank S. Karshenboim, G. Soff, and Th. Stöhlker for stimulating discussions. Financial support by DFG (Grant No. 436 RUS 113/479), by RFBR (Grant No. 98-02-04111), by GSI, and by EU-TMR program (Contract No. ERB FMRX CT 97-0144) is gratefully acknowledged.

[1] Th. Stöhlker, H. Geissel, H. Irnich, T. Kandler, C. Kozhuharov, P.H. Mokler, Münzenberg, F. Nickel, C. Scheidenberger, T. Suzuki, M. Kucharski, A. Warczak, P. Rymuza, Z. Stachura, A. Kriessbach, D. Dauvergne, B. Dunford, J. Eichler, A. Ichichara, and T. Shirai, Phys. Rev. Lett. **73**, 3520 (1994).

[2] Th. Stöhlker, C. Kozhuharov, P. H. Mokler, A. Warczak, F. Bosch, H. Geissel, R. Moshammer, C. Scheidenberger, J. Eichler, A. Ichihara, T. Shirai, Z. Stachura, and P. Rymuza, Phys. Rev. A **51**, 2098 (1995).

[3] A. Ichihara, T. Shirai, and J. Eichler, Phys. Rev. A **49**, 1875 (1994).

[4] J. Eichler and W. Meyerhof, *Relativistic Atomic Collisions* (Academic Press, San Diego, 1995).

[5] J. Eichler, A. Ichihara, and T. Shirai, Phys. Rev. A **51**, 3027 (1995).

[6] Th. Stöhlker, T. Ludziejewski, F. Bosch, R. W. Dunford, C. Kozhuharov, P. H. Mokler, H. F. Beyer, O. Brinzanescu, F. Franzke, J. Eichler, A. Griegal, S. Hagmann, A. Ichihara, A. Krämer, D. Liesen, H. Reich, P. Rymuza, Z. Stachura, M. Steck, P. Swiat, and A. Warczak, Phys. Rev. Lett. **82**, 3232 (1999).

[7] V. M. Shabaev, A. N. Artemyev, and V. A. Yerokhin, in *Trapped Charged Particles and Fundamental Physics*, edited by D. H. E. Dubin and D. Schneider (AIP, Woodbury, NY, 1999), p. 22.

[8] J. McEnnan and M. Gavrila, Phys. Rev. A **15**, 1537 (1977).

[9] D. J. Botto and M. Gavrila, Phys. Rev. A **26**, 237 (1982).

[10] V. M. Shabaev, Phys. Rev. A **50**, 4521 (1994).

[11] C. Itzykson and J.-B. Zuber, *Quantum Field Theory* (McGraw-Hill, New York, 1985).

[12] J. M. Jauch and F. Rohrlich, *The Theory of Photons and Electrons* (Springer-Verlag, Berlin, 1976).

[13] D. R. Yennie, S. C. Frautschi, and H. Suura, Ann. Phys. (N.Y.) **13**, 379 (1961).

[14] T. Beier, A. N. Artemyev, J. Eichler, V. M. Shabaev, and V. A. Yerokhin, Phys. Scr. **80**, 322 (1999).

[15] T. Beier, A. N. Artemyev, J. Eichler, V. M. Shabaev, G. Soff, and V. A. Yerokhin, Nucl. Instrum. Methods Phys. Res. B **154**, 102 (1999).

[16] V. A. Yerokhin, A. N. Artemyev, and V. M. Shabaev, Phys. Lett. A **234**, 361 (1997).

[17] A. N. Artemyev, V. M. Shabaev, and V. A. Yerokhin, Phys. Rev. A **56**, 3529 (1997); **56**, 3529 (1997).

[18] V. A. Yerokhin and V. M. Shabaev, Phys. Rev. A **60**, 800 (1999).